

# HVS-Aware Dynamic Backlight Scaling in TFT LCD's

Ali Iranli, Wonbok Lee, and Massoud Pedram  
Dept. of Electrical Engineering  
University of Southern California  
Los Angeles CA 90089

**Abstract:** Liquid Crystal Displays have appeared in applications ranging from medical equipment to automobiles, gas pumps, Laptops and handheld portable computers. These display components present a cascaded energy attenuator to the battery of handheld device which is responsible for about half of energy drain at maximum display intensity. As such, the display components become the main focus of every effort for maximization of embedded system's battery life-time. This paper proposes an approach for pixel transformation of the displayed image to increase the potential energy saving of the *backlight scaling* method. The proposed approach takes advantage of human visual system (HVS) characteristics and tries to minimize distortion between the perceived brightness values of the individual pixels in the original image and those of the backlight-scaled image. This is in contrast to previous backlight scaling approaches which simply match the luminance values of the individual pixels in the original and backlight-scaled images. Furthermore, this paper proposes a temporally-aware backlight scaling technique for video streams. The goal is to maximize energy saving in the display system by means of dynamic backlight dimming subject to a video distortion tolerance. The video distortion comprises of (1) an intra-frame (spatial) distortion component due to frame-sensitive backlight scaling and transmittance function tuning and (2) an inter-frame (temporal) distortion component due to large-step backlight dimming across frames modulated by the psychophysical characteristics of the human visual system. The proposed backlight scaling technique is capable of efficiently computing the flickering effect online and subsequently using a measure of the temporal distortion to appropriately adjust the slack on the intra-frame spatial distortion, thereby, achieving a good balance between the two sources of distortion while maximizing the backlight dimming-driven energy saving in the display system and meeting an overall video quality figure of merit. The proposed dynamic backlight scaling approach is amenable to highly efficient hardware realization and has been implemented on the Apollo Testbed II. Actual current measurements demonstrate the effectiveness of proposed technique compared to the previous backlight dimming techniques, which have ignored the temporal distortion effect.

## I. INTRODUCTION

As the portable electronic devices become more intertwined with everyday life of people, it becomes necessary to put more functionality into these devices, increase their performance, and limit their energy consumption. These devices, which are getting smaller and lighter, are often powered by rechargeable batteries. Unfortunately, the battery capacities are increasing at a much slower pace than the overall power dissipation of these devices. So it is critical to develop power-aware design methodologies and technique to bring the power dissipation growth of such devices in line with the battery capacity increase.

Major sources of power dissipation in a portable electronic device are many and vary as a function of the device functionality and performance specification. In reality, many of these devices are equipped with a Liquid Crystal Display (LCD), which tends to account for a significant portion of the total system power. For example, in the SmartBadge system, the display subsystem consumes 28.6% and 50% of the total power in the active/idle and standby modes, respectively [1]. The dominant backlighting technology for LCD's is the Cold Cathode Fluorescent Lamp (CCFL), which uses a low-voltage DC to high-voltage AC converter as the driver. This driver consumes the largest amount of power in the display subsystem.

The LCD displays currently available require two power sources, a backlight supply and a contrast supply. The display backlight is the single largest power consumer in a typical display component. Battery energy is lost in the electric-to-electric conversion to high voltage AC for driving the CCFL; where conversion efficiencies exceeding 90% are possible. Although the CCFL is the most efficient electric-to-light converter available today, it has losses exceeding 80%. Additionally, the optical transmission efficiency of present displays is under 50% for monochrome with color types much lower. Unfortunately, as for other system resources, one cannot tackle this energy hungry component with some form of power shutdown. This is due to the fact that LCD subsystem must be continuously refreshed and cannot be turned off or put to sleep without a significant penalty in performance and Quality of Service.

There are two main classes of techniques for lowering the power consumption of LCD subsystem. The first class of techniques is focused on the digital/analog interface between the graphics controller and the LCD controller. These techniques try to minimize the energy consumption by taking advantage of different encoding schemes to minimize the switching activity of the electrical bus. For instance, reference [2] uses the spatial locality of the video data to reduce the number of transition on the DVI bus reducing its energy consumption by 75%. More recently, reference [3] has extended the previous work by using the limited intra-word transition codes instead of single intra-word transition codes used in [2] and including the DC balancing conditions in the coding scheme to achieve more than 60% energy saving, on average compared to the basic transmission protocol.

The second class of techniques is focused on the video controller and the backlight to lower the energy consumption of the display system. The key idea follows from the fact that eye's perception of the light, which is emitted from the LCD panel, is a function of two parameters, 1) intensity of the backlight and 2) transmittance of the LCD panel. Thus by carefully adjusting these two parameters one can achieve the same perception in human eyes at different values of the backlight intensity and the LCD transmittance. Now because the variation in power consumption of the backlight lamp for different output luminance values is orders of magnitude larger than power consumption of the LCD panel for different pixel values, one can save energy by simply dimming the backlight and increasing the LCD transmittance to compensate for the loss of backlight luminance.

In [4], Chang et al. proposed Dynamic backlight Luminance Scaling technique (DLS) to reduce the energy consumption of the LCD displays. This approach suffers from two main drawbacks, a) it manipulates every pixel on the screen one-by-one limiting the application of this approach to still images or low-frame-rate videos; b) it achieves energy saving at the cost of loss in visual information. Reference [5] improved this simple approach by eliminating the pixel-by-pixel transformation of the displayed image through minor hardware modifications to the built-in LCD reference driver. These modifications could implement any single-band grayscale spreading function to adjust the brightness and contrast of the displayed image, extending the applicability of the approach to streaming applications. Reference [6],

proposed several approaches for power management of the display sub-system based on variable refresh rate, liquid crystal orientation shift, and backlight dimming. However, in the proposed backlight scaling technique no pixel value transformation method is used to compensate the loss of image brightness. Reference [7] proposes a display power management method based on the user's attention. In this method the display is turned off or put to sleep mode whenever a camera based image processing controller detects that the user is not looking at the screen. This method suffers from large overhead in power and performance for calculation and detection of user attention to the screen.

Reference [8] proposed a method for image transformation, whereby the dynamic range of the original image is reduced such that the incurred image distortion is no more than a pre-specified value. The authors relied on a very accurate still image quality measure. This work improved the previous methods in two key aspects. Firstly, it presented a global histogram equalization algorithm which enabled preservation of most of the visual information in spite of image transformation, and secondly, it described a simple, yet effective, modification of the architecture of built-in LCD reference driver in order to produce any piecewise linear image transformation function. The method however had two disadvantages, a) the distortion characterization curve was dependent on the displayed image; b) the equalization algorithm required histogram information of the displayed image to calculate the image transformation function. Finally, reference [9] presented a backlight scaling technique, which is based on a *tone reproduction* operator. This operator maps the original image  $\chi$  to a transformed image  $\chi'$  such that the perceived brightness of the image is preserved while its dynamic range is reduced. The operator was calculated without any information about individual pixels of the displayed image or the image histogram. The proposed method was the first to take advantage of *some* aspects of the human visual system to maximize power savings through dynamic backlight dimming (see discussions in 4.1 for details.) In addition, this method is amenable to highly efficient hardware realization because it does not require information about the histogram of the displayed image.

Although the aforementioned techniques are effective backlight scaling approaches, they all suffer from a common shortcoming, i.e., temporal blindness. All previously proposed approaches for backlight scaling have overlooked the temporal response of human visual system; more specifically they apply the backlight scaling scheme to each frame of a video sequence individually and without considering flickering effects, which may result as a consequence of frequent and abrupt changes in the backlight intensity. In the remainder of this paper, we will refer to all of the prior work techniques for video as Frame-sensitive Backlight Scaling (FBS) techniques.

In contrast, this paper proposes a backlight scaling scheme which is sensitive to the spatio-temporal information of video sequence. The key idea is to decompose the maximum allowed distortion between the original video and the backlight scaled one into two components, 1) the spatial distortion which is the intra-frame luminance distortion between the respective frames of the original and backlight scaled video sequences, and 2) the temporal distortion which is the inter-frame distortion due to (large-scale) changes of luminance over time when comparing the original and backlight scaled video sequences. In this paper, we take advantage of an analytical model of the Critical Fusion Frequency and the temporal information about the average luminance of each frame in a video sequence to capture the effect of temporal distortions incurred by backlight scaling scheme. Next, we use this information to limit the maximum allowed spatial distortion that the FBS scheme can create, and therefore, limit the overall maximum video distortion below a certain user specific limit.

In the following, the basic background on the human visual system and its temporal response, principles of photographic tone mapping, and finally the TFT LCD architecture and prior work in dynamic backlight scaling will be discussed. Next, in section III temporally-aware backlight scaling and dynamic tone mapping approach will be explained. Sections IV and V will provide the supporting experimental results and conclusions of this technique.

## II. BACKGROUND AND PRELIMINARIES

### II.A Photometric Definitions

Although light is a form of electromagnetic radiation, measurement of luminous intensity from a light source requires extra information about the relative sensitivity of the eye to different wavelengths. Photometry is the science of measuring visible light in units that are weighted according to the sensitivity of the human eye. The luminous intensity of a "white" light source is thus defined by multiplying the watts emitted at each wavelength by the efficiency of that wavelength in exciting the eye, relative to the efficiency at 555nm. This efficiency factor is referred to as the *V-lambda* curve [10]. The *candela* is the luminous intensity per solid angle, in a given direction of a source which emits monochromatic radiation at wavelength 555nm and which has a radiant intensity in that direction of 1/683 watt per steradian [11]. Humans perceive luminance, which is an approximate measure of how "bright" a surface appears when one views it from a given direction. Luminance is thus defined as luminous intensity per square meter and is measured in candela per square meter. For example, the luminance of sun, cloudy dull day, typical office, good street lighting, and full moon are 5K, 300, 15, 1.2, and 0.002cd/m<sup>2</sup>, respectively.

### II.B Human Visual System

#### II.B.1 Spatial Characteristics

When light reaches eye, it hits the photoreceptors on the retina, which then send an electrical signal through neurons to the brain where an image is formed. The photoreceptors in our retina, namely rods and cones, act as the sensors for the HVS. Rods are extremely sensitive to light and provide achromatic vision at *scotopic* levels of illumination (10<sup>-6</sup> to 10 cd/m<sup>2</sup>), that is why we cannot see colors in dark surroundings. Cones (which comprise of three distinct types) are less sensitive, but provide color vision at *photopic* levels of illumination (10<sup>-2</sup> to 10<sup>8</sup> cd/m<sup>2</sup>). Note that both rods and cones are active at light levels between 0.01 and 10 cd/m<sup>2</sup>. This range is called the *mesopic* range. The incoming light can have a dynamic range of nearly 1:10<sup>14</sup>, whereas the neurons can transfer a signal with dynamic range of only about 1:10<sup>3</sup>. The human eye can discern a dynamic range of about 10-12 orders of magnitude. As a result, there is the need for some kind of adaptation mechanism in our vision. This means that we first adapt to some (unchanging) luminance value, and then perceive images in a rather small dynamic range around this luminance value.

One of the most important characteristics that changes with different adaptation levels is the *Difference Threshold* or *Just Noticeable Difference* (JND.) The JND is the minimum amount by which stimulus intensity must be changed in order to produce a noticeable variation in sensory experience. Let  $\Delta L$  and  $L_a$  denote the JND and the adaptation luminance, respectively. Blackwell [12] showed that the ratio  $\Delta L/L_a$  varies as a function of the adaptation level,  $L_a$  and thus, established the relationship between  $L_a$  and  $\Delta L$  to be

$$\Delta L(L_a) = 0.0594 \cdot (1.219 + L_a^{0.4})^{2.5} \quad (1)$$

Simply stated, Blackwell's equation states that if there is a patch of luminance  $L_a + \epsilon$  where  $\epsilon \geq \Delta L$  on a background of luminance  $L_a$ , it will be discernible, but a patch of luminance  $L_a + \epsilon$ , where  $\epsilon < \Delta L$  will not be perceptible to the human eye.

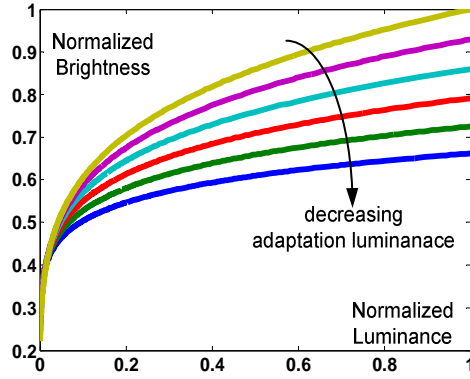


**Figure 1. Brightness vs. luminance characteristic of the HVS.**

Let us now consider the brightness perception. *Brightness* is the magnitude of the subjective sensation which is produced by visible light. Although the radiance can easily be measured, the brightness cannot exactly be quantified. Nevertheless, brightness is often approximated as the logarithm of the luminance, or the luminance raised to the power of 1/2 to 1/3 depending on the context. Studies have shown that the brightness-luminance relation depends on the adaptation level to the ambient light. In particular, Stevens et al. [13] devised the '*brils*' units to measure the subjective value of brightness. According to Stevens, one *bril* equals the sensation of brightness that is induced in a fully dark-adapted eye by a brief exposure to a 5-degree solid-angle white target of 1 micro-lambert luminance. (One lambert is equal to 3,183 cd/m<sup>2</sup>.) Let  $B$  denote brightness in *brils*,  $L$  the original luminance value in lamberts, and  $L_a$  denote the adaptation luminance of the eye. Then,

$$B = \lambda \cdot \left( \frac{L}{L_a} \right)^\sigma \quad (2-a)$$

where

$$\begin{aligned} \sigma &= 0.4 \cdot \log_{10}(L_a) + 2.92 \\ \lambda &= 10^{2.0208} \times L_a^{0.336} \end{aligned} \quad (2-b)$$

Typical perceived brightness characteristic curves are shown in Figure 1. The slope of each curve represents the *human contrast sensitivity* that is the sensitivity of the HVS brightness perception to the changes in the luminance. Note that as  $L_a$  is lowered, the human contrast sensitivity decreases. Notice also that the HVS exhibits higher sensitivity to changes in luminance in the darker regions of an image. Two images with different luminance values can result in the same brightness values, and can appear to the HVS as being identical. Actually, according to equation (2-a) we are very poor judges of an absolute luminance value; all that we can judge is the ratio of luminances, i.e. the brightness

### II.B.2 Temporal Characteristics

Studies of the dynamics of light perception can be divided into two categories based on the stimulation method utilized for the HVS characterization. The first category of techniques is based on aperiodic stimuli, which try to measure the impulse response of HVS. In these experiments, the sensitivity of the HVS is measured when a brief test light is presented to the HVS before, during, or after the presentation of a much stronger background light. The results show that the sensitivity of the HVS is at its maximum when the test light is presented during the transition of the background light [14]. Although these experiments are very effective for understanding the time domain response of the HVS, they have limited power in quantifying the distortion due to dynamic backlight scaling, which is perceived by the HVS during a video playback. This is because backlight scaling is applied to every video frame at a rate that is too fast for the HVS to settle to some steady state background brightness.

The second category of techniques tries to measure the *Critical Fusion Frequency* (CFF) of the HVS at

various *amplitude sensitivity values* (AS values.) These concepts are closely related to the well-known notion of Temporal Contrast Sensitivity Function, [15]-[17]. The CFF is the minimum frequency,  $f^*$ , above which the observer cannot detect any flickering effect when a series of light flashes at that frequency is presented to him/her, i.e., for frequencies lower than  $f^*$ , the HVS will notice the flickering. The AS at frequency  $f^*$  is the ratio of the minimum required amplitude of the flash light at frequency  $f^*$  to the average ambient luminance such that the flickering effect is perceived [14]. Generally, as the amplitude sensitivity increases, the flickering becomes easier to perceive for a series of flashes with a fixed frequency. These metrics are suitable for quantifying distortions caused by the backlight scaling since they model the “flickering” effect of periodic backlight scaling.

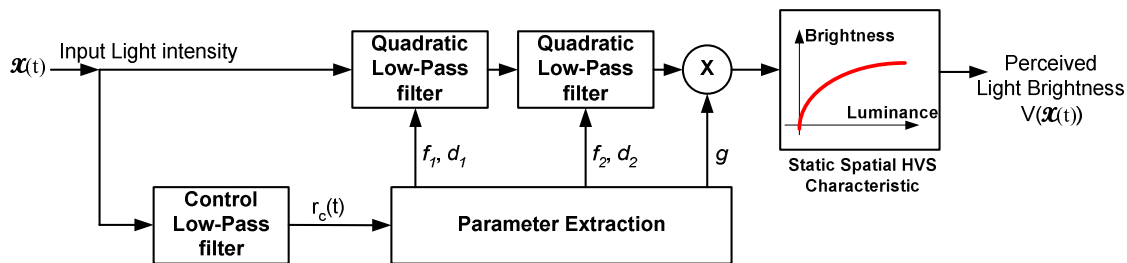


Figure 2. Temporal model of HVS

In this paper, we adopt a computational temporal response model of the HVS due to Weigand et al. [18]. Figure 2 depicts the schematic representation of this model. This model can be used to determine the AS threshold of an observer when presented with varying light intensities. Note that the input to this model is a scalar value representing the luminance of the viewing area, whereas the output is the intensity of perceived luminance. If the difference between the DC value and the amplitude of a given frequency,  $f^*$ , in the output of the model exceeds a fixed predefined threshold  $\delta$ , then the flickering is perceived by the HVS at frequency  $f^*$ . For example, in case of backlight scaling, the input to the model is the average luminance of each frame of video sequence, whereas the output of the model is the perceived intensity of the light. Basically, this model comprises of a cascade of two parametric second order low pass filters and a dynamic gain control, followed by the non-linear static characteristic of HVS which transforms the luminance values to perceived brightness values. Parameters of the two quadratic filters are controlled by a first order low pass filter with cutoff frequency near 0.1Hz.

Figure 3 shows a typical frequency domain transfer function of this model when a simple sinusoidal input with constant amplitude and varying DC value is presented to it. Note that for a fixed DC value, i.e. fixed background luminance, as we increase the frequency of the flickering light the required amplitude for the flickering to be perceived is almost constant for frequencies below 10Hz and then increases exponentially after this frequency. Moreover, for a given frequency of flashing light by increasing the background luminance the minimum amplitude of the flashing light for which the flickering is perceived decreases.

As described in [18], the control low pass filter is a first order filter with following transfer function,

$$H_{C-LP}(f) = \frac{1}{j2\pi(1.59f) + 1} \quad (3-a)$$

whereas the cascade of two quadratic low pass filters has the general transfer function of,

$$H_{LP}(f) = \left[ \frac{f_1^2}{f_1^2 + jd_1f_1f - f^2} \right] \cdot \left[ \frac{f_2^2}{f_2^2 + jd_2f_2f - f^2} \right] \quad (3-b)$$

with parameters given by,

$$\begin{aligned}
z_c(t) &= 1 / \left[ 1 + (r_c(t) / 138.839)^{0.5} \right] \\
f_1(t) &= -4.299 \cdot z_c(t) + 11.65 \\
f_2(t) &= -24.36 \cdot z_c(t) + 28.68 \\
d_1(t) &= -1.218 \cdot z_c(t) + 0.616 \\
d_2(t) &= -1.003 \cdot z_c(t) + 0.448
\end{aligned} \tag{3-c}$$

Finally, the controllable gain is given by,

$$g = 2.2 \cdot \left[ (45.899 + r_c(t))^{-0.641} \right] \cdot \left[ (0.001 + r_c(t))^{-0.5114} \right] \tag{3-d}$$

where  $r_c(t)$  is the control signal at the output of the control low pass filter given in equation (3-a) (cf. Figure 2).

It is worth noting that the models of HVS are based on subjective experiments, and therefore, their accuracy varies from one individual to next. The key idea of this paper is to underscore the significance of considering such human perceptive models during the optimization process for backlight scaling. The commercial implementation of such system can have multiple HVS models for users to select from. In section III we will take advantage of the aforementioned model and introduce a metric for measuring the distortion of original and backlight scaled video sequences in terms of incurred flickering.

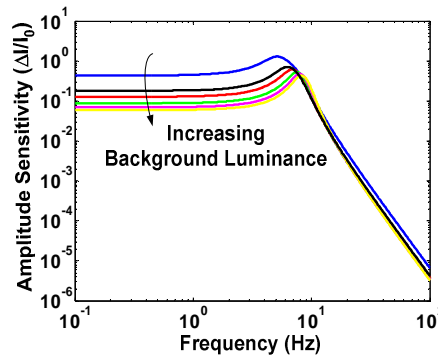


Figure 3. Sample amplitude sensitivity of HVS for sinusoidal input with varying DC value

## II.C Tone reproduction

A classic photographic task is the mapping of the potentially high dynamic range of real world luminances to the low dynamic range of the photographic print. The range of light that people experience in the real world is vast. However, the range of light one can reproduce on prints spans at best about two orders of absolute dynamic range. This discrepancy leads to the *tone reproduction* problem: how should one map measured/sensed scene luminances to print luminances and produce a satisfactory picture?

The success of photography has shown that it is possible to produce images with limited dynamic range that convey the appearance of realistic scenes. This is fundamentally possible because as mentioned in previous section human eye is sensitive to relative, rather than absolute, luminance values. Consider a typical scene that poses a problem for tone reproduction in photography, a room illuminated by a window that looks out on a sunlit landscape. A human observer inside the room can easily see individual objects in the room as well as features in the outdoor landscape. This is because the eye adapts locally as we scan the different regions of the scene. If we attempt to photograph our view, the result is disappointing. Either the window is over exposed and we can't see outside, or the interior of the room is underexposed and looks black.

In 1993, Tumblin et al. [19] introduced this concept to computer graphics community and proposed a

primitive tone mapping operator. Since then a great deal of work has been done on the tone reproduction problem. Generally speaking the tone reproduction literature can be divided into two main categories. The first category which uses a global tone mapping operator ignores the spatial information about the luminance of the original scene and adopts a single non-decreasing function as its tone mapping operator. Reference [20] uses a model of brightness perception to derive this mapping operator. Reference [21] relies on a global multiplier to maintain the visibility threshold. In reference [22] another global operator was proposed based on histogram adjustment. This method uses an image's histogram to implicitly segment the image so that separate scaling factors can be used in different luminance zones.

The second category tries to reproduce the visibility of different objects in the scene. This is done through multiple mapping functions which are adopted based on local luminance information of the original scene. Chiu et al. [23] who used a spatially varying exposure ramp over the image was the first to propose a spatially varying dynamic range reduction operator. Later work by Pattanaik et al. [24] developed the ultimate still image operator based on the human visual system, incorporating color adaptation, local contrast, and dynamic range. More recently, References [25]-[27] have proposed more successful tone mapping operators in separating the contrast differences that matter to vision from those that do not. The basic challenge for a spatially varying tone mapping operator is that it needs to reduce the global contrast of an image without affecting the local contrast to which human visual system is sensitive. To accomplish this, an operator must segment the high dynamic range image, either explicitly or implicitly, into regions that human visual system does not correlate during dynamic range reduction. Otherwise, the local varying operators would lead into disturbing "reverse gradients" typically seen as halos around light sources.

## II.D LCD architecture and Backlight Scaling

Figure 4a shows the typical architecture of the digital LCD subsystem in a microelectronic device. There are two main components in this subsystem: a) video controller and frame buffer memory and b) LCD controller and panel. The image data, which is received from the processing unit, is first saved into the frame buffer memory by the video controller and is subsequently transmitted to the LCD controller through an appropriate analog (e.g., VGA) or digital (e.g., DVI) interface.

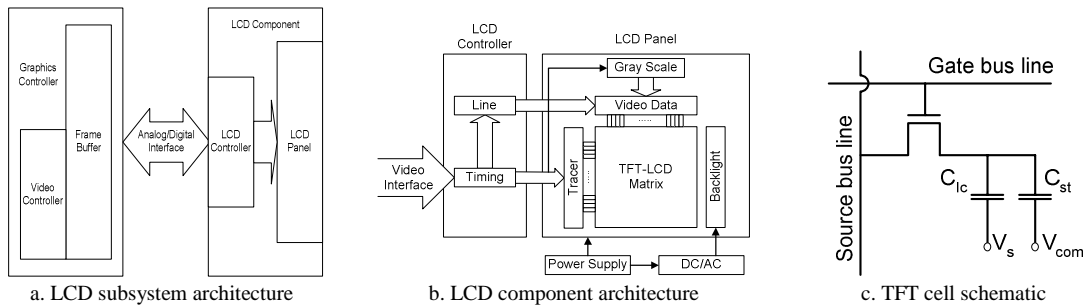


**Figure 4. TFT-LCD screen**

The LCD controller receives the video data and generates a proper grayscale – i.e., transmissivity of the panel – for each pixel based on its pixel value. All of the pixels on a transmissive LCD panel are illuminated from behind by the backlight. To the observer, a displayed pixel looks bright if its transmittance is high (i.e., it is in the 'on' state), meaning it passes the backlight. On the other hand, a displayed pixel looks dark if its transmittance is low (i.e., it is in the 'off' state), meaning that it blocks the backlight. For color LCD's, different filters are used to generate shades of three main colors (i.e. red, blue, and green), and then color pixels are generated by mixing three sub-pixels together to produce different colors.

Figure 4b depicts the LCD controller in more detail. The data received from the video bus is used to infer a row of pixels timing information and respective grayscale levels. Then, this timing information is used to select the appropriate row in the LCD matrix. Next, the pixel values are converted to the corresponding voltage levels to drive the thin-film-transistors (TFT's) on different columns of the selected row. The backlight bulb is powered with the aid of a DC-AC converter, to provide the required illumination



of the LCD matrix.

Each pixel has an individual liquid crystal cell, a TFT, and a storage capacitor (cf. Figure 4c). The electrical field of the capacitor controls the transmittance of the liquid crystal cell. The capacitor is charged and discharged by the TFT. The gate electrode of the TFT controls the timing for charging/discharging of the capacitor when the pixel is scanned (or addressed) by the tracer for refreshing its content. The (drain-) source electrode of the TFT controls the amount of charge. The gate electrodes and source electrodes of all TFT's are driven by a set of gate drivers and source drivers, respectively. A single gate driver (called a *gate bus line*) drives all gate electrodes of the pixels on the same row. The gate electrodes are enabled at the same time the row is traced. A single source driver (called a *source bus line*) drives all source electrodes of the pixels on the same column. The source driver supplies the desired voltage level (called *grayscale voltage*) according to the pixel value. In other words, ideally, the pixel value transmittance,  $t(X)$ , is a linear function of the grayscale voltage  $v(X)$ , which is in turn a linear function of the pixel value  $X$ . The transfer function of source driver which maps different pixel values,  $X$ , into different voltage levels,  $v(X)$  is called the *grayscale-voltage function*. If there are 256 grayscales, then the source driver must be able to supply 256 different grayscale voltage levels. For the source driver to provide a wide range of grayscales, a number of *reference voltages* are required. The source driver mixes different reference voltages to obtain the desired grayscale voltages. Typically, these different reference voltages are fixed and designed as a voltage divider.

Mathematically speaking, in a transmissive TFT-LCD monitor, for a pixel with value  $X$ , the luminance  $I(X)$  of the pixel<sup>1</sup> is:

$$I(X) = b \cdot t(X) \quad (4)$$

where  $t(X)$  is the transmissivity of the TFT-LCD cell for pixel value  $X$ , and  $b \in [0,1]$  is the (normalized) *backlight illumination factor* with  $b=1$  representing the maximum backlight illumination and  $b=0$  representing no backlight. Note that  $t(X)$  is a linear mapping from  $[0,255]$  domain to  $[0,1]$  range. In backlight scaled TFT-LCD,  $b$  is scaled down and accordingly  $t(X)$  is increased to achieve the same image luminance.

Let  $\mathcal{X}$  and  $\mathcal{X}' = \Phi(\mathcal{X}, \beta)$  denote the original and the transformed image data, respectively. Moreover, let  $D(\mathcal{X}, \mathcal{X}')$  and  $P(\mathcal{X}', \beta)$  denote the distortion of the images  $\mathcal{X}$  and  $\mathcal{X}'$  and the power consumption of the LCD-subsystem while displaying image  $\mathcal{X}'$  with backlight scaling factor,  $\beta$ .

**Dynamic Backlight Scaling (DBS) Problem:** *Given the original image  $\mathcal{X}$  and the maximum tolerable image distortion  $D_{max}$ , find the backlight scaling factor  $\beta$  and the corresponding pixel transformation function  $\mathcal{X}' = \Phi(\mathcal{X}, \beta)$  such that  $P(\mathcal{X}', \beta)$  is minimized and  $D(\mathcal{X}, \mathcal{X}') \leq D_{max}$ .*

The general form of DBS problem as stated above is difficult to solve due to the complexity of the distortion function,  $D$ , and also the non-linear function minimization step that is required to determine  $\Phi(\mathcal{X}, \beta)$ . From now on, in this paper we will use  $\Phi(\mathcal{X}, \beta)$  to denote the transformed image, and  $\Phi(x, \beta)$  to denote a single transformed pixel in the image  $\mathcal{X}$ .

Reference [4] describes two backlight luminance dimming techniques. Let  $x$  denote the *normalized pixel value*, i.e., assuming an 8-bit color depth,  $x = X/255$ . The authors of [4] scale the backlight luminance by a factor of  $\beta$  while increasing the pixel values from  $x$  to  $\Phi(x, \beta)$  by two mechanisms. Clearly,  $\Phi(x, \beta) = x$  denotes the identity pixel transformation function (cf. Figure 5a.) The “backlight luminance dimming with brightness compensation” technique uses the following pixel transformation function (cf. Figure 5b):

$$\Phi(x, \beta) = \min(1, x + 1 - \beta) \quad (5-a)$$

whereas the “backlight luminance dimming with contrast enhancement” technique uses this transformation function (cf. Figure 5c):

<sup>1</sup> Illuminance can be used to characterize the luminous flux emitted from a surface. Most photographic light meters measure the illuminance. In terms of visual perception, we perceive luminance. It is an approximate measure of how “bright” a surface appears when we view it from a given direction. Luminance is measured in lumens per square meter per steradian. The maximum brightness of a CRT or LCD monitor is described by luminance in its specification.

$$\Phi(x, \beta) = \min\left(1, \frac{x}{\beta}\right) \quad (5-b)$$

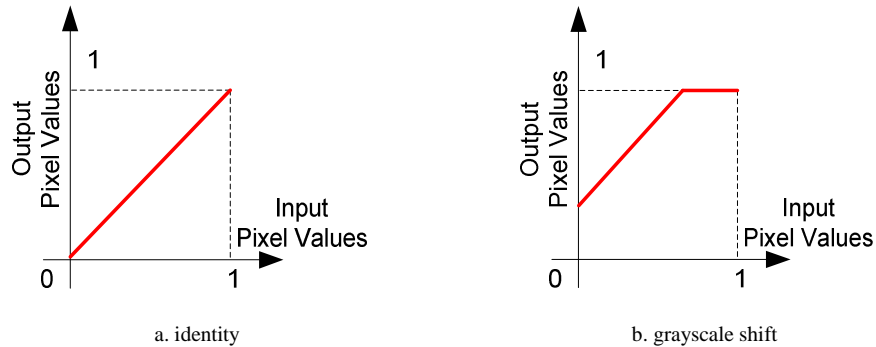
In these schemes, to calculate the distortion rate, an image *histogram estimator* is required for calculating the statistics of the input image. Note that the image histogram simply denotes the marginal distribution function of the image pixel values. Reference [4] uses the number of saturated pixel values due to aforementioned transformations as their measure of image distortion.

Reference [5] proposes a different approach in which the pixel values in both dark and bright regions of the image are used to enable a further dimming of the backlight. The key idea is to first truncate the image histogram on both ends to obtain a smaller dynamic range for the image pixel values and then to spread out the pixel values in this range (by applying an *affine transformation*) so as to enable a more aggressive backlight dimming while maintaining the contrast fidelity of the image. The pixel transformation function is given as (cf. Figure 5d):

$$\Phi(x, \beta) = \begin{cases} 0, & 0 \leq x \leq g_l \\ cx+d, & g_l \leq x \leq g_u \\ 1, & g_u \leq x \leq 1 \end{cases} \quad c = \frac{1}{g_u - g_l} = \frac{1}{\beta}; \quad d = \frac{-g_l}{g_u - g_l} \quad (6)$$

where  $(g_l, 0)$  and  $(g_u, 1)$  are the points where  $\Phi(x, \beta) = cx + d$  intersects  $\Phi(x, \beta) = 0$  and  $\Phi(x, \beta) = 1$ , respectively. In this technique the image distortion is measured based on the number of pixel values that are preserved after the application of the transformation function to the original image. The implementation of this approach is quite simple and requires minimal changes to the built-in Programmable LCD Reference Driver (PLRD). Notice that PLRD allows a class of linear transformations on the backlight-scaled image, resulting in both brightness scaling and contrast scaling. Clearly, brightness and contrast are the two most important properties of any image.

The previous approaches cannot fully utilize the power saving potential of the dynamic backlight scaling scheme, due to the fact that their measure of distortion between the original and the backlight-scaled image is an overestimation. This is because these approaches simply either minimize the number of saturated pixel values [4] or maximize the number of pixel values that are preserved [5]. The main disadvantage of these cost functions is that they treat the gray scale values in dark and white regions of the image the same way, which is in contrast to the perceived brightness characteristic of the HVS as shown in Figure 1.



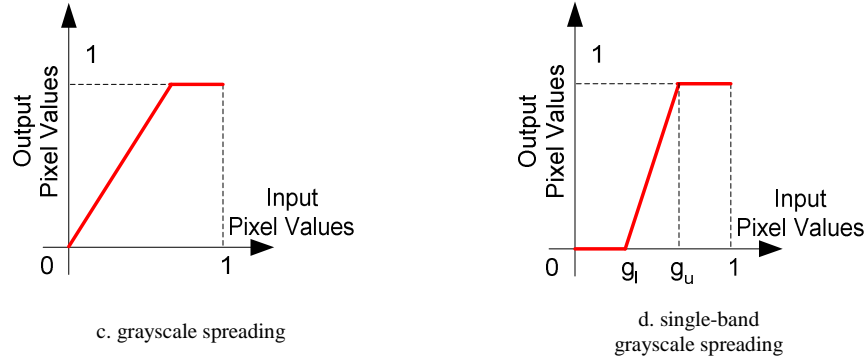


**Figure 5. Pixel transformation functions**

The aforementioned techniques for backlight scaling have proven to be quite effective for still images; however, if one tries to apply these techniques on a per-frame basis, i.e. FBS, for video streams, the output video quality may significantly be degraded. This is due to two facts: 1) they overlook a very important deciding factor in their optimization process, that is, the human visual system characteristics. All of these approaches rely on the luminance values of pixels of the displayed image as their optimization variables. However, luminance value of a light source is not the same as its perceived brightness; 2) different frames in a video clip may have different characteristics, and therefore, dynamic backlight scaling (DBS) applied in per-frame basis to a video sequence may result in different pixel transformation functions ( $\Phi$ ), and thus, different backlight scaling factors ( $\beta$ ). The abrupt changes in  $\Phi$  and  $\beta$  may result in a large flickering effect over time, which in turn adversely impacts the overall video quality.

This paper improves the previous techniques in two ways: 1) it proposes a backlight scaling technique which is based on a tone reproduction operator. This operator maps the original image  $\mathcal{X}$  to a transformed image  $\mathcal{X}'$  such that the perceived brightness of the image is preserved while its dynamic range is reduced. This reduction in the dynamic range of the image will further increase the potential for backlight scaling, and therefore, maximize the energy saving. Moreover, the proposed operator can be calculated without any information about the individual pixels of the displayed image or its histogram, further improving the video frame-rate and power savings due to elimination of any hardware/software support for image histogram generation; 2) it presents a temporally-aware backlight scaling method in which the inter-frame changes in  $\Phi$  and  $\beta$  are limited such that the perceived flickering is minimized while the maximum power saving is achieved.

### III. TEMPORALLY AWARE BACKLIGHT SCALING (TABS)

In FBS techniques, the distortion between each backlight scaled frame and the original frame, i.e. the spatial distortion, is upper bounded by a user specified maximum allowed value (cf. Figure 7). However, this spatial distortion is not sufficient to quantify the overall quality of backlight scaled video. The second component which is important in quantifying the video quality is the changes in the luminance of the backlight-scaled video compared to the original video, i.e. the temporal distortion. This component of the video distortion captures the unwanted variations in overall luminance of different frames of a backlight scaled video sequence.

Let  $\mathcal{X}$  and  $\mathcal{X}'$  denote the original and the backlight scaled versions of a video sequence with total number of frames,  $N$ . Then, we define the distortion between two video sequences  $\mathcal{X}$  and  $\mathcal{X}'$  as,

$$\begin{aligned}
 D(\mathcal{X}, \mathcal{X}') &= \alpha \cdot D_{spi}(\mathcal{X}, \mathcal{X}') + (1 - \alpha) \cdot D_{mp}(\mathcal{X}, \mathcal{X}') \\
 &= \alpha \cdot \max_i (D_{spi}(\mathcal{X}_i, \mathcal{X}'_i)) + (1 - \alpha) \cdot \frac{\sum_j (\mathcal{F}\{V(\mathcal{X})\}_j - \mathcal{F}\{V(\mathcal{X}')\}_j)^2}{\sum_j (\mathcal{F}\{V(\mathcal{X})\}_j)^2}
 \end{aligned} \tag{6}$$

where  $D_{spi}(X, Y)$  is the spatial distortion between still images,  $X$  and  $Y$ ;  $V(\cdot)$  is the perceived brightness when an input is given to the HVS (cf. Figure 2), and  $\mathcal{F}\{\cdot\}$  is the Fourier transform operator. Finally,  $\alpha$  is

the weighting coefficient. The first term in equation (6) captures the spatial distortion between the respective frames of video sequences  $\mathcal{X}$  and  $\mathcal{X}'$ , while the second term is the normalized mean square error between the spectral power density of the brightness of original video sequence and the backlight scaled one. This term, actually, captures the temporal distortion of two video sequences (cf. section II.2.B).

The video distortion function presented in equation (6) is hard to evaluate because the first term is in time domain while the second term is defined in the frequency domain. To circumvent this problem, equation (6) can be simplified using the Parseval's theorem, which simply states that integral of squared signal is equal to integral of its spectral power density, therefore,

$$\begin{aligned}
D_{mp}(\mathcal{X}, \mathcal{X}') &= \frac{\sum_j (\mathcal{F}\{V(\mathcal{X})\}_j - \mathcal{F}\{V(\mathcal{X}')\}_j)^2}{\sum_j (\mathcal{F}\{V(\mathcal{X})\}_j)^2} \\
&= \frac{\left\{ \sum_j (\mathcal{F}\{V(\mathcal{X})\}_j)^2 + \sum_j (\mathcal{F}\{V(\mathcal{X}')\}_j)^2 - 2 \sum_j (\mathcal{F}\{V(\mathcal{X})\}_j) \cdot (\mathcal{F}\{V(\mathcal{X}')\}_j) \right\}}{\sum_j (\mathcal{F}\{V(\mathcal{X})\}_j)^2} \\
&= 1 + \frac{\frac{1}{N} \sum_j (V(\mathcal{X}'_j))^2}{\frac{1}{N} \sum_j (V(\mathcal{X}_j))^2} - 2 \frac{V(\mathcal{X}) \otimes V(\mathcal{X}')}{\frac{1}{N} \sum_j (V(\mathcal{X}_j))^2} \Big|_{j=0} \\
&= 1 + \frac{\frac{1}{N} \sum_j (V(\mathcal{X}'_j))^2 - 2V(\mathcal{X}_0) \cdot V(\mathcal{X}'_0)}{\frac{1}{N} \sum_j (V(\mathcal{X}_j))^2}
\end{aligned} \tag{7}$$

Based on this video distortion measure we propose a Temporally-Aware Backlight Scaling for Video (TABS). Figure 6 shows the block diagram of this approach. The key idea is to measure the temporal distortion of backlight scaled video and then feedback this information to dynamically change the maximum allowed spatial distortion of the frames.

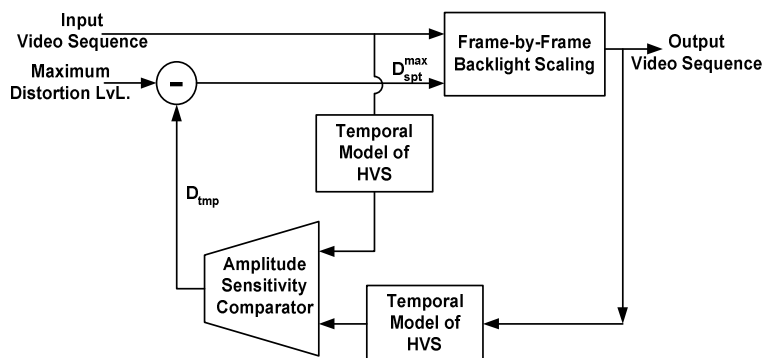


Figure 6. Temporally-aware backlight scaling

To reduce the spatial distortion between the corresponding frames of the original and backlight scaled video sequences, we propose a simple, yet effective pixel transformation function based on the static characteristic of HVS and tone mapping theory. Let  $L_{\max}$  and  $L'_{\max}$  denote the maximum luminance of the original image and the dynamically tone-mapped and backlight-scaled frame, respectively. Moreover, let  $\mathcal{X}_t$  and  $\mathcal{X}'_t$  denote the pixel value information of the original and backlight scaled frames at time  $t$ . Then, the perceived image distortion between images  $\mathcal{X}_t$  and  $\mathcal{X}'_t$  can be quantified by function  $D_{spt}(\mathcal{X}_t, \mathcal{X}'_t)$ .

**Converse Tone Mapping (CTM) Problem:** Given an original image  $\mathcal{X}_t$  and maximum allowable image distortion  $D_{max}$ , find the tone mapping operation  $\psi : [0, L_{\max}] \rightarrow [0, L'_{\max}]$  such that  $L'_{\max}$  is minimized while

$$D_{spt}(\mathcal{X}_t, \mathcal{X}'_t) \leq D_{max} \tag{8}$$

where  $\mathcal{X}' \equiv \psi(\mathcal{X})$ .

The aforementioned problem is the converse of the tone mapping problem, because in the tone

mapping problem, the goal of optimization is to find the mapping operator  $\Psi$  such that for a given maximum display luminance, the image distortion is minimized [19]. In contrast, in the CTM problem, the goal of optimization is to find the minimum of maximum luminance value that guarantees a given maximum image distortion level. Unfortunately, due to complexity of HVS, and therefore the complexity of the image distortion function,  $D_{sp}$ , neither the CTM problem nor the tone mapping problem have closed form solutions.

To solve the CTM problem, this paper proposes a heuristic approach based on *pixel brightness preservation*. The key idea is to make sure that the JND in the backlight scaled image and that in the original image are equal. In this way, the image perception is preserved, i.e., both images have the same discernible details.

Mathematically speaking, let  $L_a$  and  $L'_a$  denote the adaptation luminance for the original and the backlight scaled images. Based on equation (1), the JND for the original image is  $\Delta L(L_a)$  and the JND for the backlight scaled image will be  $\Delta L(L'_a)$ . Therefore, to preserve the discernible details of the image, we ought to find a tone mapping function,  $\Psi$ , such that,  $\Delta L(L'_a) = \psi(\Delta L(L_a))$ .

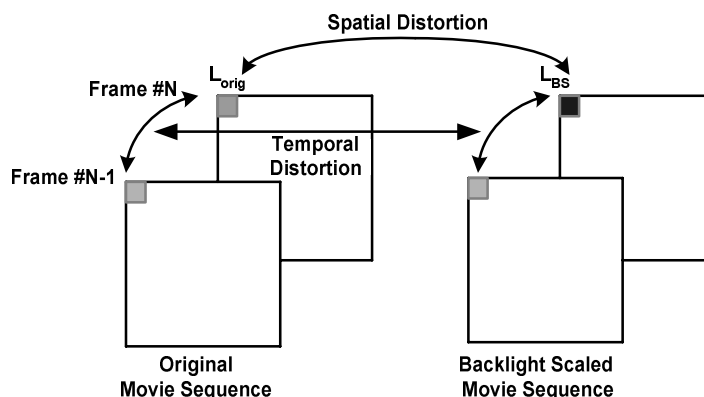


Figure 7. Spatial vs. Temporal distortions

As a simple solution, one can assume a variable scaling function where the scaling factor changes depending upon the local luminance value. Subsequently, the lighter regions of the image will be scaled more non-linearly than the darker regions so as to take advantage of the decreasing human contrast sensitivity from dark to light regions of the image (cf. Sec. II.B.1) However, this approach requires manipulation of individual pixel values, which may be undesirable for real-time implementation. Therefore, this paper first adopts  $\Psi$ , to be a constant scaling function  $\psi(x) = \kappa \cdot x$ , where  $\kappa$  can be calculated from equation (1). Consider two pixels in the original image,  $x_1$  and  $x_2$ , which are discernible therefore,  $x_1 - x_2 = \Delta L(L_a)$ . If we want to preserve the discernible details of the image in the transformed image we need to have  $\psi(x_1) - \psi(x_2) = \Delta L(L'_a)$ , substituting the pixel transformation function with  $\psi(x) = \kappa \cdot x$  one can calculate the  $\psi$  as a function of  $L_a$  and  $L'_a$ ,

$$\begin{aligned}
\psi(x_1) - \psi(x_2) &= \Delta L(L'_a) \\
\kappa \cdot (x_1 - x_2) &= \Delta L(L'_a) \\
\kappa \cdot \Delta L(L_a) &= \Delta L(L'_a) \\
\kappa &= \frac{\Delta L(L'_a)}{\Delta L(L_a)} \\
\kappa &= \left( \frac{1.219 + (L'_a)^{0.4}}{1.219 + (L_a)^{0.4}} \right)^{2.5}
\end{aligned} \tag{9}$$

where  $L_a$  and  $L'_a$  may be approximated by half of the maximum backlight luminance before and after backlight scaling, i.e.,  $0.5L_{\max}$  and  $0.5L'_{\max}$ . Please note that the adaptation luminance level,  $L_a$ , (cf. section II.B.1) is a key parameter in determining the perception of brightness. There are many techniques available for measuring the ambient light, e.g. by means of light sensors. However, these techniques are power consuming and use up resources. In this paper, for our experimental results, we use a simple method for approximating the ambient light as one half of the maximum luminance of the display system itself. Our approach can be easily modified to consider any form of adaptation luminance (ambient light) measurement or estimation.

Equation (9) represents the key difference between our approach and those reported previously in references [4]-[8]. In those approaches,  $\kappa$  is essentially set as  $L'_{\max} / L_{\max}$  in order to preserve the pixel luminance values, whereas in our approach  $\kappa$  is given by equation (9). In addition, to capture the human contrast sensitivity (cf. Sec. II.B.1, Figure 1), we will use a functional form for the transformation function,  $\Psi$ , which is similar to that of the human brightness perception function, i.e. (cf. eqn. 2),

$$\psi(\mathcal{X}) = \kappa(L_a, L'_a) \cdot \left( \frac{\mathcal{X}}{L_a} \right)^{\gamma(L_a, L'_a)} \tag{10}$$

where  $\kappa(L_a, L'_a)$  is simply the luminance intensity adjustment factor as given by equation (9) and  $\gamma(L_a, L'_a)$  is the human contrast sensitivity change between the original image and the backlight scaled image, that is,

$$\gamma(L_a, L'_a) = \frac{\sigma}{\sigma'} \tag{11}$$

The motivation behind introduction of parameter  $\gamma(L_a, L'_a)$  is to affect large and small luminance values differently. More precisely, if only the  $\kappa(L_a, L'_a)$  factor was used, in the transformed backlight scaled image the contrast between two pixels would have been increased uniformly with respect to that of the original image; however, with introduction of  $\gamma(L_a, L'_a)$ , as the contrast between two pixels in the original image increases the contrast between same two pixels in the backlight scaled image would increase but, grow more slowly for smaller pixel luminance values. Therefore, the result would be a single tone mapping function which takes into account the sensitivity saturation of HVS (cf. Figure 1.)

To measure the temporal distortion,  $D_{\text{tmp}}$ , of the video sequence we use the following procedure,

1. For each original frame,  $\mathcal{X}_t$ , and backlight scaled frame,  $\mathcal{Y}_t$ , at time  $t$ , calculate the mean brightness value,  $\bar{\mathcal{X}}(t)$  and  $\bar{\mathcal{Y}}(t)$  of all pixels in the respective frames.
2. Filter signals  $\bar{\mathcal{X}}(t)$  and  $\bar{\mathcal{Y}}(t)$ , using the temporal response model of HVS to get perceived luminance signals  $\bar{\mathcal{X}}_{\text{HVS}}(t)$  and  $\bar{\mathcal{Y}}_{\text{HVS}}(t)$ , respectively.
3. Calculate equation (7) for  $\bar{\mathcal{X}}_{\text{HVS}}(t)$  and  $\bar{\mathcal{Y}}_{\text{HVS}}(t)$  to get  $D_{\text{tmp}}$ .

Next, we use  $D_{\text{tmp}}$  to modify the maximum allowed spatial distortion,  $D_{\text{spt}}^{\max}$ , in FBS techniques (cf.

Figure 6.)

## IV. IMPLEMENTATION AND EXPERIMENTAL RESULTS

### IV.A Hardware characterization

#### IV.A.1 Cold Cathode Fluorescent Lamp (CCFL)

The CCFL illumination is a complex function of the driving current, ambient temperature, warm-up time, lamp age, driving waveform, lamp dimensions, and reflector design [28]. In the transmissive TFT-LCD application, only the driving current is controllable. Therefore, we model the CCFL illumination as a function of the driving current only and ignore the other parameters. Accounting for the saturation phenomenon in the CCFL light source [29], we use a two-piece linear function to characterize the power consumption of CCFL as a function of the backlight factor:

$$P_{backlight}(\beta) = \begin{cases} A_{lin} \cdot \beta + C_{lin} & 0 \leq \beta \leq C_s \\ A_{sat} \cdot \beta + C_{sat} & C_s < \beta \leq 1 \end{cases} \quad (12)$$

Relationship between the CCFL illumination (i.e., luminous flux incident on a surface per unit area) and the driver's power dissipation for the CCFL in LG Philips transmissive TFT-LCD LP064V1 [30] is shown in Figure 8.a. The CCFL illumination increases monotonically as the driving power increases from 0 to 80% of the full driving power. For values of driving power higher than this threshold, the CCFL illumination starts to saturate. The saturation phenomenon is due to the fact that the increased temperature and pressure inside the tube adversely impact the efficiency of emitting visible light [31].

After interpolation, we obtain the following coefficient values for the CCFL in LG Philips transmissive TFT-LCD LP064V1:

$$C_s=0.8234, A_{lin}=1.9600, C_{lin}=-0.2372, A_{sat}=6.9440, \text{ and } C_{sat}=-4.3240.$$

#### IV.A.2 TFT-LCD display matrix

The hydrogenated amorphous silicon (a-Si:H) is commonly used to fabricate the TFT in display applications. For a TFT-LCD panel, the a-Si:H TFT power consumption can be modeled by a quadratic function of pixel value  $x \in [0,1]$  [32]

$$P_{TFT\ Panel}(x) = a \cdot x^2 + b \cdot x + c \quad (13)$$

We performed the current and power measurements on the LG Philips, LP064V1 LCD. The measurement data are shown in Figure 6b. The regression coefficients are thus determined as:

$$a=0.02449, b=-0.04984, \text{ and } c=0.993.$$

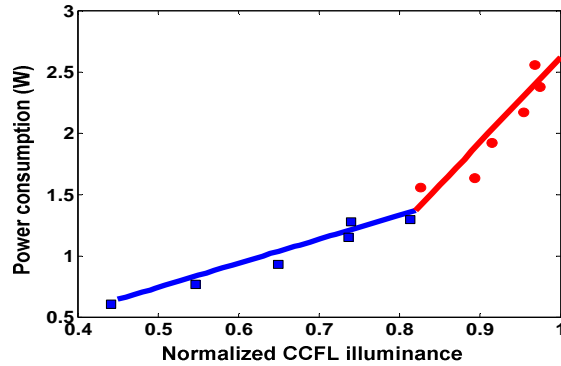
Normally white TFT-LCD panel consumes less power while displaying brighter (luminance-enhanced) image. Thus, this type of panel adds additional power saving to the backlight scaling technique because it generally enhances the luminance of the image that is displayed on the panel to compensate for the loss of the brightness after backlight dimming. In contrast, power consumption of normally black TFT-LCD panel increases slightly as its global transmittance increases (which increases power savings of a backlight dimming approach.) However, for either type of the TFT-LCD, the change in power consumption as a function of the transmittance is so small that it can be ignored.

#### IV.A.3 Image distortion characterization

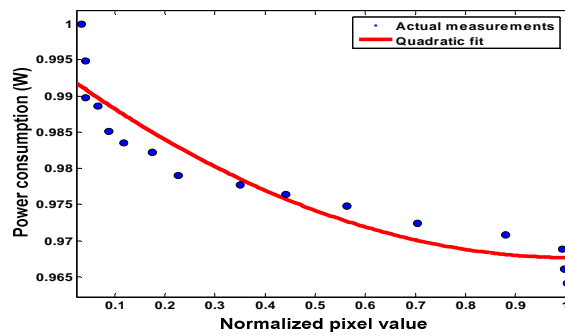
To deal with the complexity of image distortion function,  $D$ , first the image distortion function is characterized for a set of benchmark images as a function of the dynamic range of the tone-mapped images. Next standard curve fitting tools are used to generate an empirical image distortion curve based on this data. Finally, this empirical curve is utilized as the image distortion function  $D$  to find the minimum required dynamic range for any given image to achieve the maximum image distortion of  $D_{max}$  after tone-mapping.

We adopted the *universal image quality index* proposed in [33] as our distortion measure and used a set of benchmark images from the USC SIPI Image Database (USID) [34]. The USID is considered the de-

-facto benchmark suite in the signal and image processing research field [35]. Figure 9 depicts the resulting distortion values for these images when the dynamic range of the transformed image is set to twelve different values. Figure 10 is a subset of benchmarks reported to provide a visual reference for the distortion measure. Next, we used standard curve fitting tools provided in MATLAB version 7 release 14 to find the best “average” and “worst-case” global fits to these distortion values. The result is an empirical curve depicted in Figure 9, which maps target dynamic range of transformed images to the observed distortion values.



a. CCFL illuminance (i.e., backlight factor  $b$ ) versus driver's power consumption for a CCFL source



b. Pixel transmittance, versus power consumption of a pixel in the normally white TFT-LCD panel

**Figure 8. LCD Component Power Consumption Characterization**



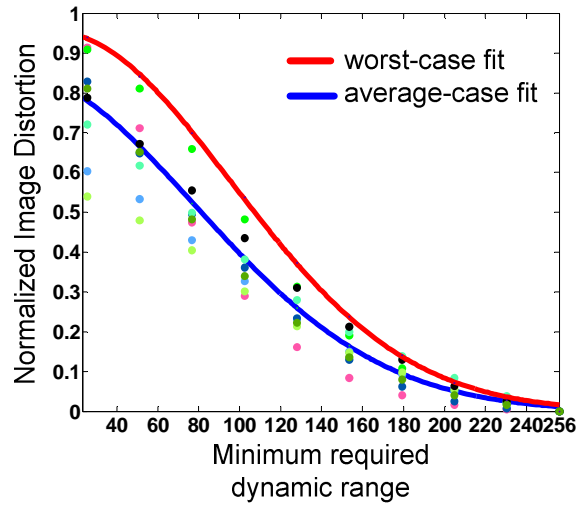


**Figure 9. Image distortion vs. Dynamic Range**

Original	Dynamic range=200	Dynamic range = 150	Original	Dynamic range=200	Dynamic range = 150
Normalized power =1	Distortion=4.3% Power saving=36.19%	Distortion=10.6% Power saving=45.24%	Normalized power =1	Distortion=5% Power saving=35.72%	Distortion=12% Power saving=46.49%
Normalized power =1	Distortion=3.3% Power saving=37.16%	Distortion=7.4% Power saving=48.28%	Normalized power =1	Distortion=3.6% Power saving=32.21%	Distortion=5.1% Power saving=42.57%

**Figure 10. Sample images and their corresponding transformed versions**

#### IV.B Implementation

To generate the experimental results we used a setup as shown in Figure 11. The Apollo test-bed II is used as the experimental platform [36]. This test-bed uses Intel X-scale 80200 processor and includes different peripheral devices such as, video capture device, GPS, and 802.11a wireless connection. Moreover, this test-bed has a 6.4" LCD screen with 6 bit/color/pixel at 640x480 resolution, and provides enough hardware/software capabilities for changing the intensity of the backlight and online calculation of the image histogram. The processor runs at 733MHz and at this speed can decode and play MPEG-1 video stream at the rate of 15 frames per second. We modified the MPEG-1 decoder application to incorporate the FBS backlight scaling technique based on the tone mapping function described in Section III.

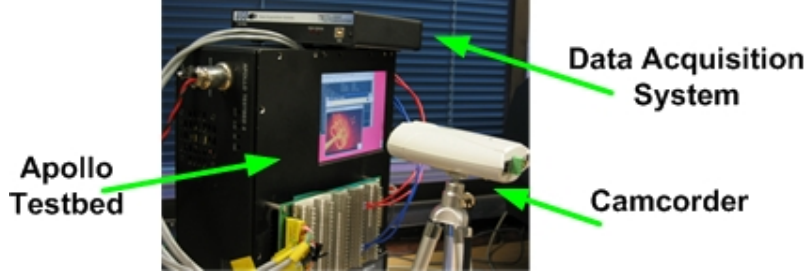


Figure 11. Experimental Setup

To implement the proposed temporally-aware backlight scaling, we made two observations, 1) the HVS model presented in section II.B.2 is a continuous-time model while the average luminance of each frame in the displayed video is calculated on frame by frame basis, resulting in a discrete-time signal. Therefore, we transformed the continuous-time filters given by equations (1-a, d) to discrete-time filters. 2) the output of the control low-pass filter in Figure 2 does not change significantly. This is due to limited range of output luminance values for typical off-the-shelf LCD. Therefore, we assumed the output of control filter to be constant, i.e.,  $rc(t)=r_0$  (cf. Figure 2). This assumption results in a fixed quadratic filters and gain blocks in the temporal model of the HVS.

Using these observations and calculating the output of the control low-pass filter,  $r_0$ , we get the following digital filter,

$$H_{LP}(f) = \left[ \frac{0.017}{1.067 - 2.05z + z^2} \right] \cdot \left[ \frac{0.011}{1.05 - 2.03z + z^2} \right] \quad (14)$$

Next, we implemented this digital filter and then calculated the output of the HVS model for the average luminance value of each frame in the video sequence.

For the online calculation of the temporal distortion,  $D_{imp}$ , we approximated the average value calculated in equation (7), by averaging the signal over limited number of previous filtered average luminance values, i.e., approximating the overall average by a moving average. Then, we used this value and the user specified maximum allowed video distortion,  $D_{max}$ , in equation (6) to calculate the maximum allowed spatial distortion,  $D_{spt}^{max}$ . Next, we use  $D_{spt}^{max}$  as the constraint for the proposed tone mapping based backlight scaling to calculate the pixel transformation function for the original image with dynamic range  $DR$ . To calculate the pixel transformation function we first lookup the corresponding allowed dynamic range,  $DR'$ , for the given  $D_{spt}^{max}$  using the distortion curves in Figure 9, and then calculate the pixel

transformation function using equation (10). This is done by calculating  $L'_a$  as  $L'_a = L_a \cdot \frac{DR'}{DR}$ . Then, we

apply the calculated transfer function using a technique similar to reference [8].

#### IV.B.1 Static Measurements

To show the effectiveness of proposed tone mapping based pixel transformation function, we measured the power saving for different still images from USC SIPI database. The results are shown in table 1. These power savings are generated for three different values of distortion levels. Clearly, by increasing the maximum tolerable distortion level the power saving should increase, which is also confirmed with listed results. Please note that the average power saving of 45% is achieved only for mere distortion level of 10%. This is about 10% increase in power saving comparing to the results reported in [4] and [5].

Name	Power saving (%)		
	Distortion = 5%	Distortion = 10%	Distortion = 20%

Lena	37.43	49.28	59.52
Autumn	35.16	49.20	61.53
Football	36.62	45.85	55.57
Peppers	36.60	44.34	56.55
Greens	35.33	45.26	53.58
Pears	37.51	47.16	54.49
Onion	34.26	48.21	60.53
Trees	36.69	44.31	54.62
West	38.52	51.18	57.50
Pout	32.57	43.22	49.54
Sail	32.33	39.18	46.51
Splash	36.55	47.20	53.53
Girl	36.45	45.30	52.52
Baboon	39.52	46.10	52.51
TreeA	31.53	40.98	49.52
HouseA	35.49	48.15	53.48
GirIB	35.65	51.28	52.59
Testpat	37.53	48.22	53.54
Elaine	36.33	45.18	55.50
<b>Average</b>	35.88	46.16	54.38

**Table 1. Power saving for different distortion levels**

#### IV.B.2 Temporal Measurements

In our experiments, to capture the temporal behavior of proposed approach and to measure the overall video quality, we ran each movie clip three different times and recorded the output of the LCD display using a camcorder at the rate which was four times faster than the displayed frame rate. At the same time, the power consumption of the LCD component was recorded using a high-speed Data Acquisition System (DAQ). In the first run, we tried an original video sequence without any backlight scaling scheme; in the second run, we applied the backlight scaling scheme to each frame independently, and finally in the third run we applied the TABS technique.

To measure the video distortion due to temporal variations of the backlight and the pixel transformation function, we calculated the average luminance value for each of the recorded frames to get the time domain signal for the spatial average luminance of pixels. Next, we calculated the HVS response to this signal by using the discrete-time domain filter given in equation (14) and then, plotted the frequency domain representation of the output.

Figure 12 compares the temporal behavior of the three different movie clips for different maximum allowed distortion rates. Note that for each movie clip, the output of Histogram Equalization for Backlight Scaling (HEBS) method proposed in [8] has a number of unwanted strong low frequency components, which cause unwanted flickering, whereas the temporally-aware backlight scaling scheme (TABS) has a frequency domain characteristic almost identical to the original sequence. Moreover, as we increase the maximum allowed video distortion the amplitude of different frequencies significantly increases for HEBS, whereas the amplitude of the TABS remains almost unchanged. Note that the amplitude of each frequency captures the effective perceived flickering at that frequency. Table 2 summarizes these results in terms of incurred temporal distortion with more than 25% improvement on average comparing to HEBS for 5% video distortion. Figure 13 depicts the time domain variations of the backlight scaling factor for the first

movie clip. As expected, compared to HEBS, TABS results in smoother backlight variations. Figure 14 shows the overall energy savings of the LCD for different movie clips and different backlight scaling schemes. As expected HEBS achieves higher energy savings since it does not consider the temporal distortion of the video sequence. However, the loss in energy savings due to consideration of the temporal distortion in the TABS scheme is not significant whereas the overall video quality is significantly improved as depicted in Figure 12. Moreover, as we increase the overall maximum allowed video distortion the difference between the energy savings of HEBS and TABS schemes become smaller. This is due to the fact that for larger video distortion values the temporal distortion contributes less to the overall distortion, whereas for smaller video distortions contributes more.

Furthermore, by increasing the overall maximum allowed video distortion the LCD energy savings is increased in both cases, which implies the obvious tradeoff between the energy consumption and the video quality.

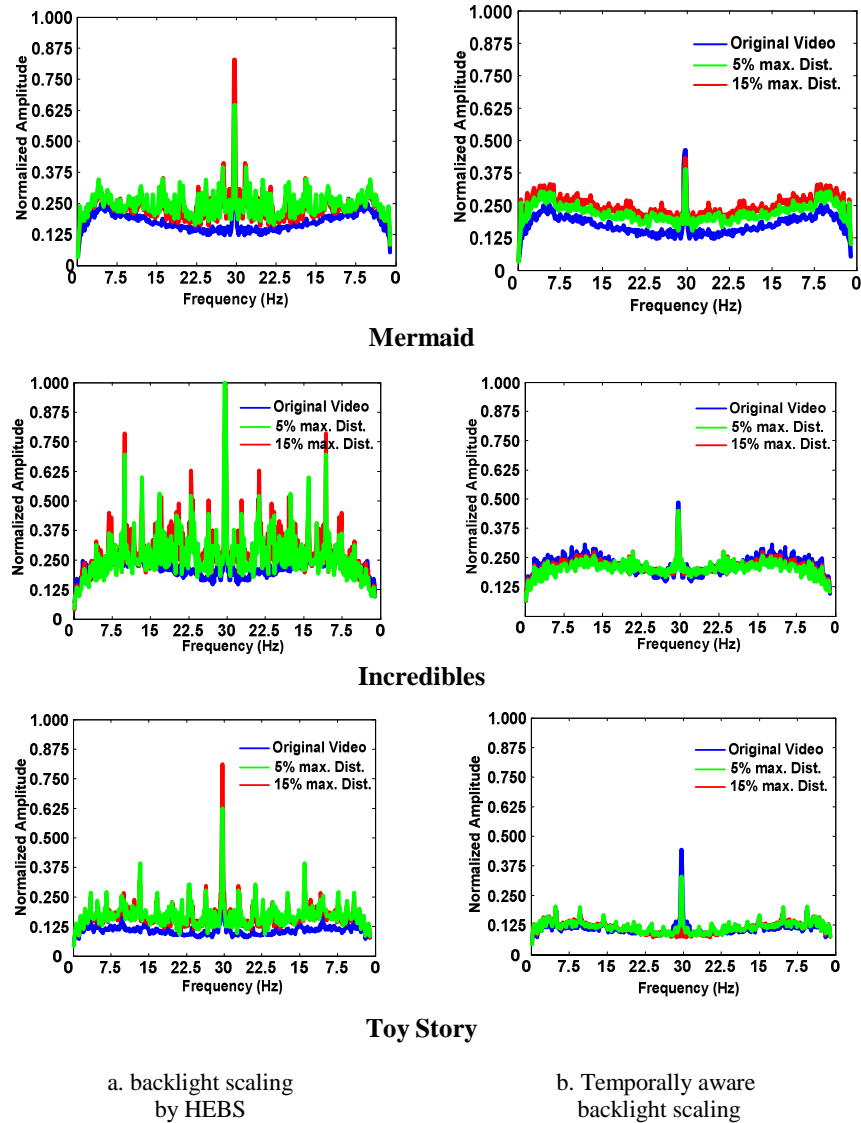


**Figure 12. Fourier transform of output video sequence**

Video Sequence	Temporal Distortion (%)			
	5% video distortion		15% video distortion	
	TABS	HEBS	TABS	HEBS
Mermaid	1.48	18.23	3.82	23.74
Incredibles	4.03	43.12	5.35	68.27
Toy Story	2.43	28.67	3.36	34.57
Average	2.64	30.06	4.17	42.20

Table 2. Comparison of temporal distortion, TABS vs. HEBS

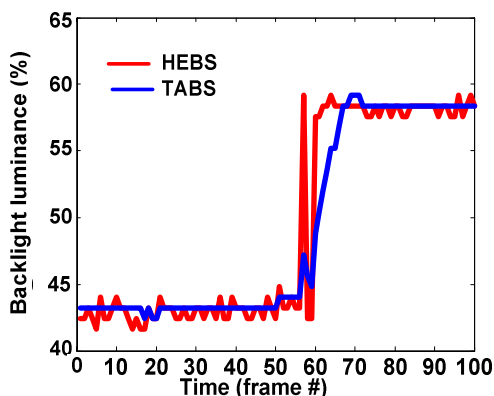


Figure 13. Time domain variations of backlight luminance

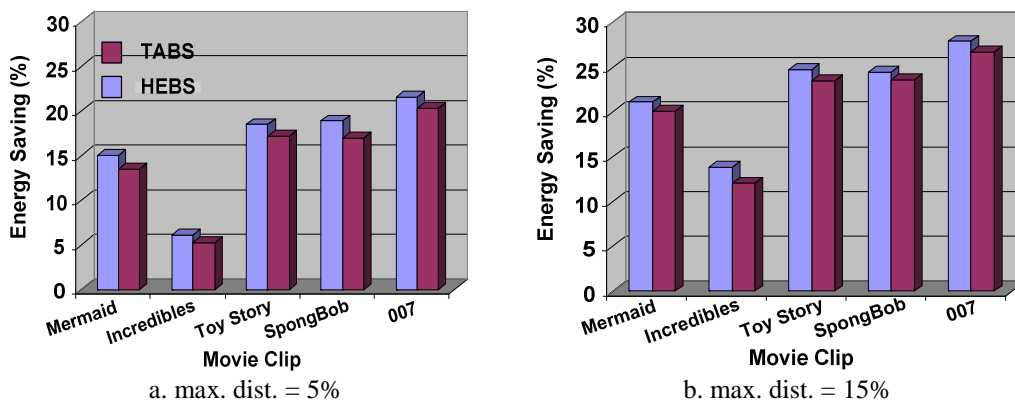


Figure 14. Energy saving – Temporally aware vs. frame-sensitive

## V. CONCLUSIONS

LCD's have appeared in applications ranging from medical equipment to automobiles, gas pumps, Laptops and handheld portable computers. These display components present a cascaded energy attenuator to the battery of handheld device which is responsible for about half of energy drain at maximum display intensity. As such, the display components have become the main focus of efforts for maximization of embedded system's battery life-time. The goal of dynamic backlight scaling (DBS) is to reduce the energy consumption of the LCD's. This paper introduced new techniques for pixel transformation of the displayed image to increase the potential energy saving of the backlight scaling techniques. These techniques take advantage of the human visual system characteristics to minimize distortion between the original and backlight-scaled still images or video sequences. The long-term impact of this research work is to

significantly reduce the power consumption of typical handheld devices, increasing the typical battery lifetime, thereby, enabling more widespread and convenient use of such devices. The backlight dimming technology can also be applied in AC-powered systems where the key concern is the energy cost to the individual user as well as the society at large. This technology has the potential to reduce the typical energy bill of a desktop computer by 30% or so (when the system is being used).

## VI. REFERENCES

- [1] T. Simunic et al., "Event-driven power management," IEEE Tran. Computer-Aided Design of Integrated Circuits and Systems, vol. 20, pp. 840-857, July 2001.
- [2] W-C. Cheng and M. Pedram, "Chromatic Encoding: a Low Power Encoding Technique for Digital Visual Interface." IEEE Transactions on Consumer Electronics, Vol. 50, No. 1, Feb. 2004, pp. 320-328.
- [3] S. Salerno, A. Bocca, E. Macii, M. Poncino, "Limited Intra-Word Transition Codes: An Energy-Efficient Bus Encoding for LCD Interfaces," Proc. of ISLPED, Aug. 2004, pp. 206-211.
- [4] N. Chang, I. Choi, H. Shim, "DLS: Dynamic Backlight Luminance Scaling of Liquid Crystal Display," IEEE Transactions on Very Large Scale Integration Systems, Vol. 12, No. 8, Aug. 2004, pp.837-846.
- [5] W-C. Cheng and M. Pedram, "Power Minimization in a Backlit TFT-LCD by Concurrent Brightness and Contrast Scaling," IEEE Transactions on Consumer Electronics, Vol. 50, No. 1, Feb. 2004, pp. 25-32.
- [6] F. Gatti, A. Acquaviva, L. Benini, B. Ricco, "Low Power Control Techniques For TFT LCD Displays," Proceedings of the 2002 international conference on Compilers, architecture, and synthesis for embedded systems, Grenoble, France, pp 218-224, 2002, ACM Press.
- [7] V. G. Moshnyaga, E. Morikawa, "LCD Display Energy Reduction by User Monitoring," Proceedings of the 2005 International Conference on Computer Design, Vol. 00, pp- 94-97, 2005, IEEE Computer Society.
- [8] A. Iranli, Hanif Fatemi, M. Pedram, "HEBS: Histogram Equalization for Backlight Scaling," Proc. of Design Automation and Test in Europe, Feb. 2005.
- [9] A. Iranli, M. Pedram, "DTM: Dynamic Tone Mapping for Backlight Scaling," Proc. of Design Automation Conference, Jun. 2005.
- [10] ANSI/IES. 1986. Nomenclature and Definitions for Illuminating Engineering, ANSI/IES RP-16-1986. New York, NY: Illuminating Engineering Society of North America.
- [11] Ian Ashdown, *Radiosity: A Programmer's Perspective*, © October 2002 by Heart Consultants Limited. (Originally published by John Wiley & Sons in 1994.)
- [12] H.R. Blackwell, "Contrast thresholds of human eye," Journal of Optical Society of America, No. 36, Vol. 11, Nov. 1946.
- [13] S. S. Stevens, J. C. Stevens, "Brightness Function: Effects on Adaptation", Journal of Optical Society of America, vol. 53, No. 3, pp. 375-385, Mar. 1963
- [14] Graham, N. and Hood, D., "Modeling the dynamics of light adaptation: The merging of two traditions," Vision Research, 32, 1373-1393, 1992
- [15] B.H. Crawford, "Visual adaptation in relation to brief conditioning stimuli," Proc. of the Royal Society, B 134, 283-302.
- [16] G.M. Shickman, "Visual masking by low-frequency sinusoidally modulated light," Journal of the Optical Society of America, 60, 107-117.
- [17] D.C. Hood, "Lower-level visual processing and models of light adaptation," Annual Review of Psychology, 49, 503-535.
- [18] Wiegand, T.E., Hood, D.C., and Graham, N., "Testing a computational model of light-adaptation dynamics," Vision Research., 35, 21, 3037-3051, 1995.
- [19] J. Tumblin, H. Rushmeier, "Tone reproduction for computer generated images," IEEE Computer Graphics and Applications, Vol, 13, No. 6, Nov. 1993, pp42-48.
- [20] J.A.Ferwerda, S.N.Pattanaik, P. Shirley, D.P.Greenberg, "A model of visual adaptation for realistic image synthesis," Proc. SIGGRAPH 1996, ACM SIGGRAPH: Addison Wesley.

- [21] G. Ward, "A contrast-based scalefactor for luminance display," Graphics Gem IV, P. Heckbert Ed., Cambridge.
- [22] L. Ward, H. Rushmeier, C. Piatko, "A visibility matching tone reproduction operator for high dynamic range scenes," IEEE Transactions on Visualization and Computer Graphics, Vol.3, No. 4, Oct. 1997, pp.291-306
- [23] K. Chiu, M. Herf, P. Shirley, S. Swamy, C. Wang, and K. Zimmerman, "Spatially Non-uniform Scaling Function for High Contrast Images," Proc. Graphics Interface, MAY 1993.
- [24] S.N. Pattanaik, J.A. Ferwerda, M.D. Fairchild, D. Greenberg, "A multiscale model of adaptation and spatial vision for realistic image display", Proc. ACM SIGGRAPH, 1998, pp.287-298.
- [25] M. Ashikhmin, "A tone mapping algorithm for high contrast images," Proc. of Eurographics Workshop on Rendering, 2002.
- [26] P. Choudhury, J. Tumblin, "The trilateral filter for high contrast images and meshes," In Proc. of the Eurographics Symposium on Rendering, 2003, pp.186-196.
- [27] F. Durand, J. Dorsey, "Fast bilateral filtering for display of high-dynamic-range images," ACM Transactions of Graphics, Vol.21, No.3, 2002, pp.257-266.
- [28] J. Williams, "A fourth generation of LCD backlight technology," Linear Technology Application Note 65, Nov. 1995.
- [29] W-C. Cheng and M. Pedram, "Transmittance scaling for reducing power dissipation of a backlit TFT-LCD," In Ultra Low-power Electronics and Design, Edited by Enrico Macii, Kluwer Academic Publisher, June 2004.
- [30] LG Philips, LP064V1 Liquid Crystal Display.
- [31] Stanley Electric Co., Ltd., [CFL] cold cathode fluorescent lamps, 2003.
- [32] H. Aoki, "Dynamic characterization of a-Si TFT-LCD pixels," HP Labs 1996 Technical Reports (HPL-96-19), February 21, 1996.
- [33] Zhou Wang and Alan C. Bovik, "A Universal Image Quality Index," IEEE Signal Processing Letters, vol. 9, no. 3, March, 2002.
- [34] A. G. Weber, "The USC-SIPI image database version 5," USC-SIPI Report #315, Oct. 1997. Also <http://sipi.usc.edu/services/database/Database.html>.
- [35] Digital Image Processing, William K. Pratt, Third Edition, John Wiley & Sons, 2003.
- [36] <http://apollo.usc.edu/testbed/>
- [37] Z. Wang, A. C. Bovik, H. R. Sheikh, and E. P. Simoncelli, "Image quality assessment: From error visibility to structural similarity," IEEE Transactions on Image Processing, vol. 13, no. 4, pp.600-612, Apr. 2004.
- [38] P.C. Teo and D.J. Heeger, "Perceptual image distortion," ISET/SPIE's Symposium on Electronic Imaging: Science and Technology, 1994.
- [39] Analog Devices, AD8511 11-Channel, Muxed Input LCD Reference Drivers.